RESEARCH

Open Access

Harnessing redox proteomics to study metabolic regulation and stress response in lignin-fed *Rhodococci*

Xiaolu Li[1,2†], Austin Gluth[1†], Song Feng[2], Wei-Jun Qian[2] and Bin Yang[1,2*]

Abstract

Background *Rhodococci* are studied for their bacterial ligninolytic capabilities and proclivity to accumulate lipids. Lignin utilization is a resource intensive process requiring a variety of redox active enzymes and cofactors for degradation as well as defense against the resulting toxic byproducts and oxidative conditions. Studying enzyme expression and regulation between carbon sources will help decode the metabolic rewiring that stymies lignin to lipid conversion in these bacteria. Herein, a redox proteomics approach was applied to investigate a fundamental driver of carbon catabolism and lipid anabolism: redox balance.

Results A consortium of *Rhodococcus* strains was employed in this study given its higher capacity for lignin degradation compared to monocultures. This consortium was grown on glucose vs. lignin under nitrogen limitation to study the importance of redox balance as it relates to nutrient availability. A modified bottom–up proteomics workflow was harnessed to acquire a general relationship between protein abundance and protein redox states. Global proteomics results affirm differential expression of enzymes involved in sugar metabolism vs. those involved in lignin degradation and aromatics metabolism. As reported previously, several enzymes in the lipid biosynthetic pathways were downregulated, whereas many involved in β-oxidation were upregulated. Interestingly, proteins involved in oxidative stress response were also upregulated perhaps in response to lignin degradation and aromatics catabolism, which require oxygen and reactive oxygen species and generate toxic byproducts. Enzymes displaying little-to-no change in abundance but differences in redox state were observed in various pathways for carbon utilization (e.g., β-ketoadipate pathway), lipid metabolism, as well as nitrogen metabolism (e.g., purine scavenging/synthesis), suggesting potential mechanisms of redox-dependent regulation of metabolism.

Conclusions Efficient lipid production requires a steady carbon and energy flux while balancing fundamental requirements for enzyme production and cell maintenance. For lignin, we theorize that this balance is difficult to establish due to resource expenditure for enzyme production and stress response. This is supported by significant changes to protein abundances and protein cysteine oxidation in various metabolic pathways and redox processes.

Keywords Lignin degradation, *Rhodococcus*, Redox biology, Proteomics, Metabolic regulation

---

†Xiaolu Li and Austin Gluth contributed equally to this work.

*Correspondence:
Bin Yang
bin.yang@wsu.edu
Full list of author information is available at the end of the article

Li *et al. Biotechnology for Biofuels and Bioproducts*   (2023) 16:180

Page 2 of 13

Background

Bacteria of the genus *Rhodococcus* are promising microbial chassis for synthesis of fuels and chemicals using low-cost biomass derived substrates. They are well-known for their ligninolytic capabilities and capacity to produce lipids, which are valuable platform chemicals [1–3]. Under stressful conditions such as nitrogen limitation, oleaginous *Rhodococci* such as *R. jostii* RHA1 and *R. opacus* PD630 accumulate triacylglycerides (TAG) using certain carbon sources. To date research into the fundamentals of bacterial TAG synthesis has focused on carbohydrate utilization and the metabolic rearrangements implicated in supplying metabolic precursors and NADPH for lipogenesis [4–7]. Questions pertaining to the feasibility of lipid production using lignin, aromatics, and non-sugar compounds (e.g., furfural) have persisted [8–10]. Compared to lipid production using lignin model compounds or carbohydrates, *Rhodococci* grown on lignin produce substantially less lipids [11–13]. Lignin utilization is a resource intensive process exemplifying a costly tradeoff between enzyme production and cell biomass accumulation to maintain a balance between supplies and energy required for catabolism (oxidation) and those for anabolism (reduction).

Lignin is a complex heterogeneous polymer comprised of various aromatic subunits linked together by C–O–C and C–C bonds. A broad repertoire of redox active and accessory enzymes are employed for lignin depolymerization and aromatics metabolism [14]. *Rhodococci* express various peroxidases and accessory oxidases to depolymerize lignin. For example, *R. jostii* RHA1 employs the well-characterized dye-decolorizing peroxidase (DypB) [15]. DypB is a versatile lignin peroxidase that requires peroxide for activity and directly uses phenolics and manganese ions as free radical mediators for lignin degradation. Following depolymerization, upper pathways funnel a wide variety of aromatics to the central aromatic intermediates catechol, protocatechuate, and gallate [16]. *R. opacus* PD630 and *R. jostii* RHA1 use β-ketoadipate, phenylacetic acid, and other central pathways to aerobically cleave aromatics and ultimately produce central metabolites [9].

Co-cultivation of different microbial strains can enhance utilization of biomass-derived substrates for improved growth and bioproduct synthesis [17]. Compared to monocultures, a consortium of *Rhodococci* showed a higher capacity to degrade alkali lignin from corn stover potentially due to enzymatic synergism [9, 18]. Engineered *R. jostii* deficient in vanillate O-demethylase (VanA⁻) was employed to funnel lignin-derived aromatics to vanillate, which can hypothetically be used for lipid production by *R. opacus* [18–20]. Nevertheless, lignin to lipid yields for the consortium were

comparable to those of monocultures [8]. Proteomics analysis was subsequently conducted to elucidate the molecular mechanisms conferring the emergent property of increased lignin degradation and to explore differences in the expressed metabolism of glucose-fed vs. lignin-fed cultures [9]. Pathways related to carbohydrate metabolism, including glycolysis, the pentose phosphate (PP) pathway, and the Entner–Doudoroff (ED) pathway, were greatly downregulated using lignin as the sole carbon source under nitrogen limitation. These pathways can provide NADPH, glycerol 3-phosphate, and acetyl-CoA for TAG synthesis [4, 21]. Fatty acid β-oxidation was likely upregulated to produce NADH and acetyl-CoA for growth as well as enzymes for lignin utilization. TAG synthesis enzymes were largely downregulated during lignin fermentation [9].

Reactive oxygen species (ROS) such as hydrogen peroxide (H_2O_2) are implicated in lignin and aromatics utilization [22, 23]. Interestingly, antioxidant enzymes are upregulated during lignin utilization: these include thioredoxin, catalase, and superoxide dismutase, which compete with fatty acid synthesis for NADPH [9, 24]. Lipid metabolism is intrinsically tied to the redox state of *Rhodococcus* [4, 25, 26]. Costa et al. reported a group of fatty acid synthesis proteins that were differentially oxidized at cysteine thiols [4]. Thiol redox post-translational modifications (PTM) can alter protein activities to regulate biological processes and/or protect against oxidative damage [27–30]. Redox PTMs generally occur as reversible oxidation of cysteine thiol groups and include S-mycothionylation (SSM), S-sulfenylation (SOH), disulfide bonds, etc. [25, 31]. The regulatory interplay between lignin catabolism, oxidative stress, and lipid metabolism is still uncharacterized. We hypothesize that redox-dependent mechanisms modulate carbon metabolism. To address this, a LC–MS/MS-based proteomics approach was applied to measure protein abundance and cysteine thiol oxidation (i.e., protein redox state) in the same experiment [32]. The redox proteomes of a *Rhodococcus* consortium were quantitatively compared for glucose vs. lignin growth conditions—providing the first, direct evidence of redox-dependent PTMs as a function of carbon source.

Results

Protein abundance patterns during cultivation on lignin vs. glucose
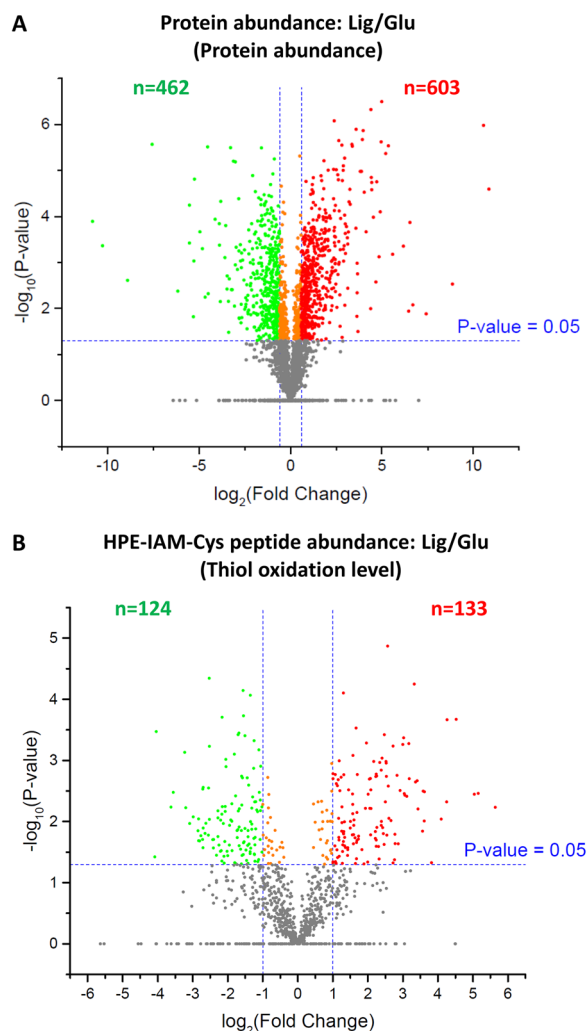
A recently reported LC–MS/MS-based direct detection workflow was adapted for this study to simultaneously quantify protein abundances and protein cysteine thiol oxidation [32]. This is accomplished by omitting enrichment steps for cysteine-containing peptides. This analytical approach was used to study

a *Rhodococcus* synthetic consortium (*R. jostii* RHA1, *R. opacus* PD630, and *R jostii* RHA1 VanA⁻) grown on 5 g/L glucose or lignin as the sole carbon source under nitrogen-limitation [9, 32]. Following cell lysis, reduced cysteine free thiols were blocked with the alkylation agent HPE-IAM to minimize oxidation during sample preparation (Fig. 1A). Oxidized thiol PTMs including disulfide (S−S), SSM, SO_2H, and SO_3H are comparably stable under mild conditions, mostly preserving them during sample preparation [27]. In contrast to the published direct detection method, which focused on exploring multiple types of cysteine PTMs, this study harnesses the MS intensities of HPE-IAM alkylated cysteine-containing peptides (HPE-IAM-Cys) to determine protein oxidation level. Proteins were considered as "having lower oxidation levels" when the corresponding HPE-IAM-Cys peptides were detected with higher MS intensities (Fig. 1B). In total 3682 proteins were identified using our LC−MS/MS workflow. A higher coverage of protein identification and quantification was achieved compared to the previous label-free proteomic analysis using filter-aided sample preparation [9]. Compared to the glucose condition, 603 proteins were upregulated and 462 proteins downregulated in the lignin condition (fold-change > 1.5, Student's *t*-test *q*-value < 0.05) (Fig. 2A).
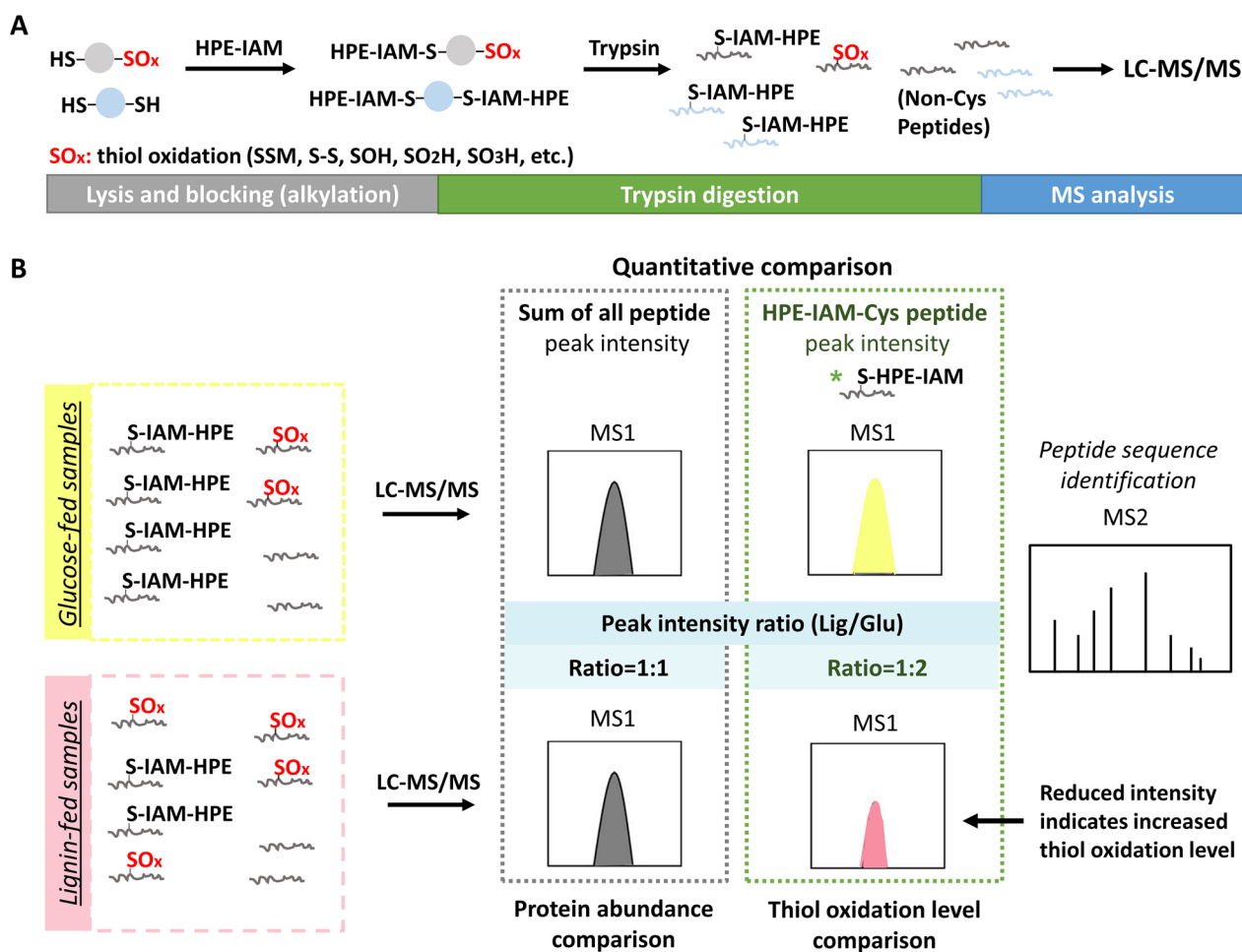
Fig. 1 Quantification of protein abundance and cysteine thiol oxidation levels in *Rhodococci* fed on glucose or lignin as sole carbon sources. **A** Proteomics sample preparation. Proteins were extracted in the presence of HPE-IAM. Cysteine free thiols (SH) were alkylated with HPE-IAM while oxidized cysteine residues (e.g. SOH, SSM, S−S, SO_2H, SO_3H) were preserved. Then, proteins were digested for MS analysis. **B** Simultaneous relative quantification of protein abundance and thiol oxidation level. Peptide samples from glucose- or lignin-fed *Rhodococci* were subjected to MS analysis. The sum of MS1 peak intensities of all peptides assigned to individual proteins were used to compare a given protein's abundance between two conditions. The peak intensities of HPE-IAM alkylated Cys-containing (HPE-IAM-Cys) peptides were summed for individual protein Cys residues, showing the abundance of protein cysteines at reduced state, which can be used to compare the thiol oxidation level of a given Cys site between two conditions. Note that the assay provides an indirect measurement of thiol oxidation level. The higher intensities of HPE-IAM-Cys peptides indicate lower cysteine thiol oxidation levels and vice versa

Li *et al. Biotechnology for Biofuels and Bioproducts*   (2023) 16:180

Page 4 of 13

A

Protein abundance: Lig/Glu
(Protein abundance)

B

HPE-IAM-Cys peptide abundance: Lig/Glu
(Thiol oxidation level)

Fig. 2 Relative quantification of protein abundance and HPE-IAM-Cys peptide abundance (i.e. cysteine thiol oxidation level). **A** Volcano plot comparing protein abundances in *Rhodococci* samples during lignin vs. glucose fermentations. Proteins with significantly changed abundances were indicated in red (upregulated) or green (downregulated). Criteria was applied: adjusted *p*-value < 0.05, fold-change > 1.5. **B** Volcano plot comparing cysteine thiol oxidation levels of individual proteins in *Rhodococci* samples for the aforementioned conditions. Protein cysteine sites with significantly altered oxidation levels were indicated in red (reduced oxidation) or green (increased oxidation). Criteria was applied: adjusted *p*-value < 0.05, fold-change > 1.5

Consistent with our previous findings, enzymes involved in lignin depolymerization and upper aromatics pathways were observed (Additional file 1: Table S1). This includes the peroxidase DypB; however, significant differences in abundance were not observed likely because the secretomes were not analyzed [15]. Cytochrome P450 (CYP) was also observed but only in the lignin condition. This heme-thiolated monooxygenase is involved

in demethylation and/or dealkylation of alkoxybenzoates such as guaiacol [33]. In *R. rhodochrous*, CYP is part of a two-component system with two redox partners, ferredoxin and ferredoxin reductase (upregulated up to 21.5-fold in our results) [34]. The products of this reaction are catechol and formaldehyde—the latter being an example of a toxic byproduct generated during lignin degradation. Enzymes in central aromatic degradation pathways including the β-ketoadipate pathway (both catechol and protocatechuate branches), phenylacetic acid pathway, and homogentisate pathway were significantly upregulated (up to 14.9-fold) in the lignin condition. Catechol 2,3-dioxygenase and 2-keto-4-pentenoate hydratase, which catalyze meta-cleavage of catechol, were upregulated.

Enzymes that produce and cycle reactive oxidants to attack lignin via Fenton chemistry were also upregulated in *Rhodococci* [35, 36]. These include glycolate oxidase, quinone reductases (up to 28.7 fold), NAD(P)H dehydrogenase, and cholesterol oxidase [37–42]. Glycolate oxidase is a flavin mononucleotide (FMN)-dependent enzyme that catabolizes phenylglyoxal and mandelic acid substrates as well as toxic glycolaldehyde byproducts [40]. Expression of these enzymes as well as the generation of toxic byproducts from lignin degradation may partially explain the upregulation of oxidative stress response proteins including catalases, alkyl hydroperoxide reductases, and a cold shock protein [25, 43]. Some proteins involved in the synthesis and degradation of mycothiol (MSH, a low-molecular-weight antioxidant) were also more abundant [44]. Corroborated by the results of Hensen et al., a MSH-dependent enzyme crucial for detoxifying formaldehyde, a byproduct of guaiacol and vanillin catabolism, was upregulated 3.8 fold. This dehydrogenase produces S-formylmycothiol and NADPH [23]. These results suggest competing NADPH requirements between lignin utilization and lipogenesis. In accordance with lignin depolymerization, proteins involved in central aromatic degradation pathways including the β-ketoadipate pathway (both catechol and protocatechuate branches), phenylacetic acid pathway, and homogentisate pathway were significantly upregulated (up to 14.9-fold) in the lignin condition. Catechol 2,3-dioxygenase and 2-keto-4-pentenoate hydratase, which catalyze meta-cleavage of catechol, were upregulated.

In addition to their structural role, lipids are secondary metabolites crucial for redox homeostasis and energy balance [26]. Plausibly induced by redox imbalance, enzymes involved in lipid metabolism were differentially expressed [25]. A number of proteins involved in β-oxidation were significantly upregulated (e.g., acetyl-CoA C-acyltransferase, upregulated up to 72.5 fold) during lignin conversion. A few proteins involved in fatty

Li *et al. Biotechnology for Biofuels and Bioproducts*   (2023) 16:180

Page 5 of 13

acid synthesis were upregulated in the lignin condition: these include FabG, a 3-oxoacyl-[acyl-carrier-protein] reductase; FabD, an [acyl-carrier-protein] S-malonyltransferase, and FabF, a 3-oxoacyl-[acyl-carrier-protein] synthase. These enzymes are components of the type II Fatty Acid Synthase (FAS-II), which elongates acyl-CoA to produce mycolic acids [45, 46]. Mycolic acids are characteristic constituents of Mycobacterial cell walls and modulate cell surface properties in response to the environment and stressors—including aromatics [47]. Several acyltransferases of the Kennedy pathway were downregulated, which supports the negligible lipid accumulation observed during lignin utilization. Glyceroneogenesis enzymes including glycerol-3-phosphate dehydrogenase were also downregulated.

Differences in protein cysteine oxidation according to carbon source

To evaluate protein redox states, we utilized an indirect approach whereby alkylated peptides would indicate original levels of reduced cysteine free thiols. Proteins assigned with higher intensities of HPE-IAM-Cys peptides (i.e., reduced Cys-containing peptides) were considered as having lower oxidation levels. Selection criteria were applied for both statistical significance (Student's *t*-test *q*-value < 0.05) and fold change (at least 1.5-fold changes to HPE-IAM-Cys peptide intensities) (Fig. 2B). In total, 1668 alkylated cysteine-containing peptides were quantitatively compared. 133 HPE-IAM-Cys peptides showed higher abundance (i.e., lower oxidation levels) while 124 cysteine sites had higher oxidation levels for lignin vs. glucose fermentations. Some cysteine residues were represented by several HPE-IAM-Cys peptides, which requires additional data processing to faithfully represent the redox state for a given residue. Thus, protein redox states were further analyzed at the Cys site level by annotation and aggregation of the raw intensities of HPE-IAM-Cys peptides. The summed intensities of individual protein Cys sites were compared by Student's t-test. Protein Cys sites with significantly changed oxidation level were filtered by: fold-change > 1.5, Student's *t*-test raw *p*-value < 0.05. To differentiate redox state changes from protein abundance, only proteins with insignificant differences in abundance (− 1.5 < protein abundance fold-change < 1.5) were considered as candidates regulated according to their redox state. 162 differently oxidized protein Cys sites passed our criteria. These proteins were mainly involved in carbohydrate metabolism, lignin/aromatic degradation, lipid metabolism, stress response, amino acid metabolism, and energy balance (Fig. 3).

Without glucose or other sugars as carbon sources, a group of proteins involved in carbon metabolism (e.g.,

glycolysis and aromatics catbolism) were more oxidized during lignin fermentation: these include catechol 1,2-dioxygenase (CatA), fructose-bisphosphate aldolase (FBA), and phosphoglucomutase (PGM) (Fig. 3A). CatA is important for aromatics catabolism; it uses molecular oxygen and a non-heme reaction center for intradiol cleavage of catechol [48]. The oxidized Cys67 site is found in its conserved linker domain, which is involved in homodimerization according to protein sequence classification using InterPro and a structural analysis of a related species [49, 50]. It is possible that oxidized Cys67 affects the conformation of this domain and, as a result, phospholipid binding, dimerization, protein complex localization, and/or other functions; however, there are no other reports of this cysteine residue in literature. In yeast, FBA is partially oxidized during oxidative stress, thus affecting a variety of cellular pathways [51]. In *actinobacteria*, redundant FBA activity was observed suggesting a cycle between gluconeogenesis as well as the Entner–Doudoroff and pentose phosphate (PP) pathways [52, 53]. In contrast, malate synthase (MLS) was less oxidized, which may affect metabolic flux through the glyoxylate cycle, and thus the production of succinate and malate for gluconeogenesis (Fig. 3B). Pentose phosphate (PP) pathway enzymes F420-dependent glucose-6-phosphate dehydrogenase (FGD), and xylulokinase (XLK) were less oxidized (Figs. 3B and 4). Besides its obvious role in sugar metabolism, the PP pathway is crucial for coping with oxidative stress and provides intermediates for fatty acid synthesis [3]. FGD is reportedly involved in an F420-depedent anti-oxidant mechanism for bacterial stress response [54].

An enzyme central to energy metabolism, dihydrolipoamide dehydrogenase (DLDH), showed decreased oxidation levels for Cys42 and Cys47 during lignin conversion (6.37-fold change in intensity). DLDH is ubiquitous for its role as a subunit of the pyruvate dehydrogenase complex, α-keto glutarate dehydrogenase complex, and branched chain amino acid dehydrogenase complex—many of which require the antioxidant cofactor α-lipoic acid [55]. The DLDH catalytic mechanism involves NAD^+ reduction and $FADH_2$ oxidation cycles for cysteine disulfide bond formation [56, 57]. According to UniProt, Cys42 and Cys47 are within the active site and tend to form a redox-sensitive disulfide bond [58]. The activity of this protein is reversibly altered by H_2O_2 and reducing agents [59]. Recently, Rahmanpour et al. reported that DLDH in *Thermobifida fusca* prevented in vitro lignin re-polymerization [60]. The capture of reduced DLDH during lignin conversion suggests a multifaceted role in ROS scavenging, lignin degradation, and/or redox regulation of central metabolism.

Li *et al. Biotechnology for Biofuels and Bioproducts*   (2023) 16:180

Page 6 of 13
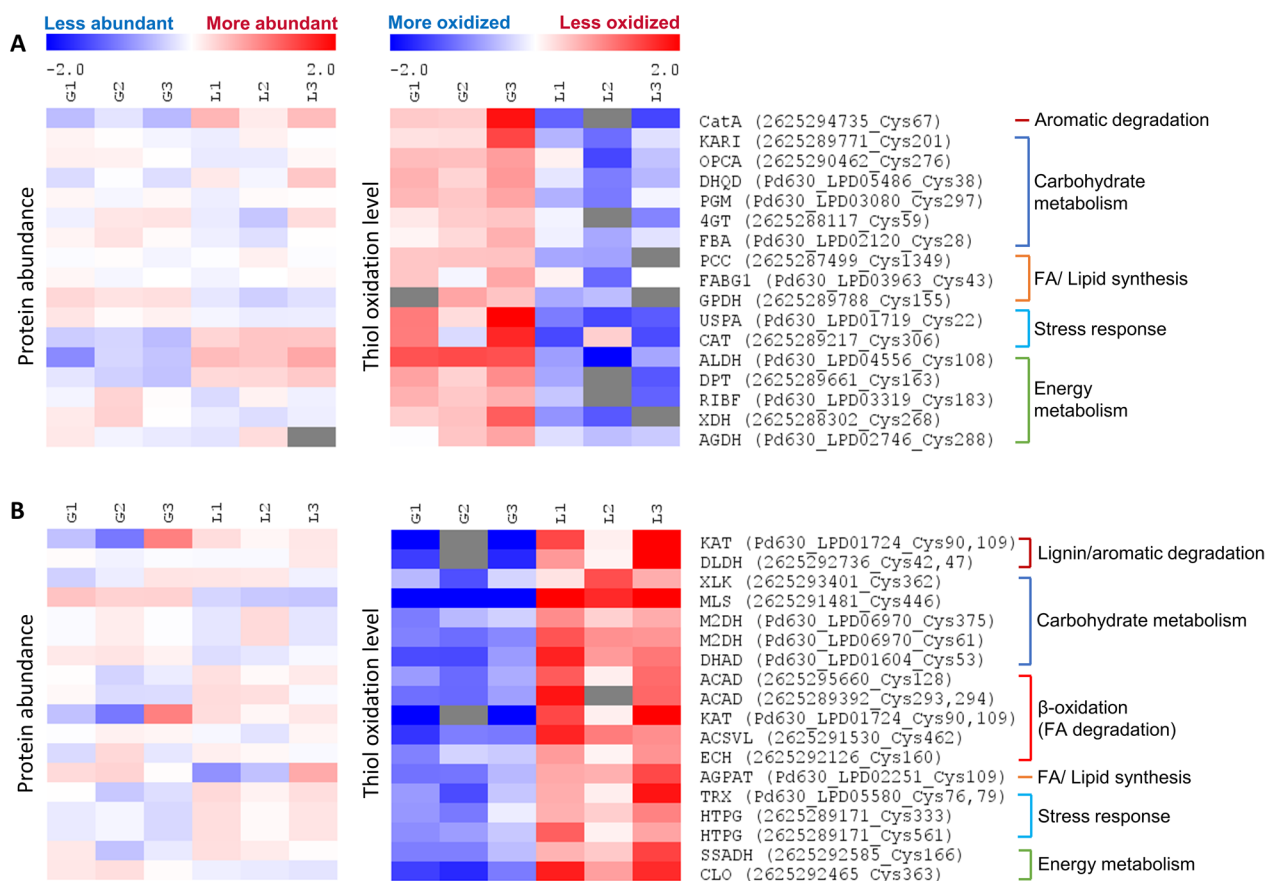
Fig. 3 Overview of the differentially oxidized protein at cysteine site level (*p*-value < 0.05, and fold-change ≥ 1.5) among the lysate samples from glucose or lignin fermentation after 5 days. The ID prefixes correspond to the following: "Pd630" = *R. opacus* PD630 and "26,252…" = *R. jostii* RHA1. Left panel: protein abundance level; right panel: protein cysteine thiol oxidation level. Relative abundances (intensities) of proteins or HPE-IAM-Cys peptides were log2 transformed and median centered to zero. Each row represents one protein Cys site and each column represented one sample. "G1", "G2" and "G3" are the lysate triplicate samples from glucose fermentation; "L1", "L2" and "L3" are the lysate triplicate samples from lignin fermentation. All the fermentation was conducted by co-culture of three strains: *R. jostii* RHA1, *R. jostii* RHA1 vanA⁻, *R. opacus* PD630. The protein name abbreviation was followed by FASTA IDs of strains and Cys site IDs. **A** The selected proteins more oxidized during lignin fermentation. **B** The selected proteins more reduced during lignin fermentation

The redox states of certain cysteine residues for enzymes involved in anabolism were also quantified. Two enzymes involved in fatty acid synthesis displayed increased oxidation in the lignin condition (Fig. 3A): acetyl/propionyl-CoA carboxylase alpha unit (ACC/PCC) and another component of FAS-II, a 3-oxoacyl-[acyl-carrier-protein] reductase (FabG1). ACC/PCC is involved in de novo fatty acid synthesis. In *S. cerevisiae*, this protein's enzymatic activity can be attenuated in a redox-controlled fashion [51]. In *E. coli*, redox-sensitive components of FAS-II (e.g., FabF) were oxidized during nitrosative stress [61]. Interestingly, both these proteins are less oxidized during nitrogen-limitation (supporting TAG accumulation) compared to nitrogen abundance (limiting TAG accumulation) in *R. jostii* RHA1 [4]. In this study, *Rhodococci* were grown in nitrogen-limited conditions; nevertheless, using lignin as the sole carbon source

still led to a significant shift towards oxidized fatty acid synthesis enzymes. Ultimately, a reduced state may be required for carbon flux to lipids.

Two acyl-CoA dehydrogenases (ACAD) were less oxidized in lignin-fed *Rhodococci* samples. ACAD catalyzes the first step in each cycle of β-oxidation to break down fatty acids. In eukaryotes, there is evidence suggesting that the activity of this enzyme is decreased due to cysteine PTMs (e.g., oxidation, alkylation, etc.): it is possible that this regulatory mechanism is conserved in prokaryotes [62, 63]. Furthermore, a 3-ketoacyl-CoA thiolase (ACAA/KAT), which catalyzes the thiolytic cleavage of 3-ketoacyl-CoA into acyl-CoA and acetyl-CoA during β-oxidation, was also less oxidized (18.5-fold higher intensity of HPE-IAM-Cys peptides) during lignin fermentation. Notably, ACAA/KAT also catalyzes the last step of β-ketoadipate pathway converting
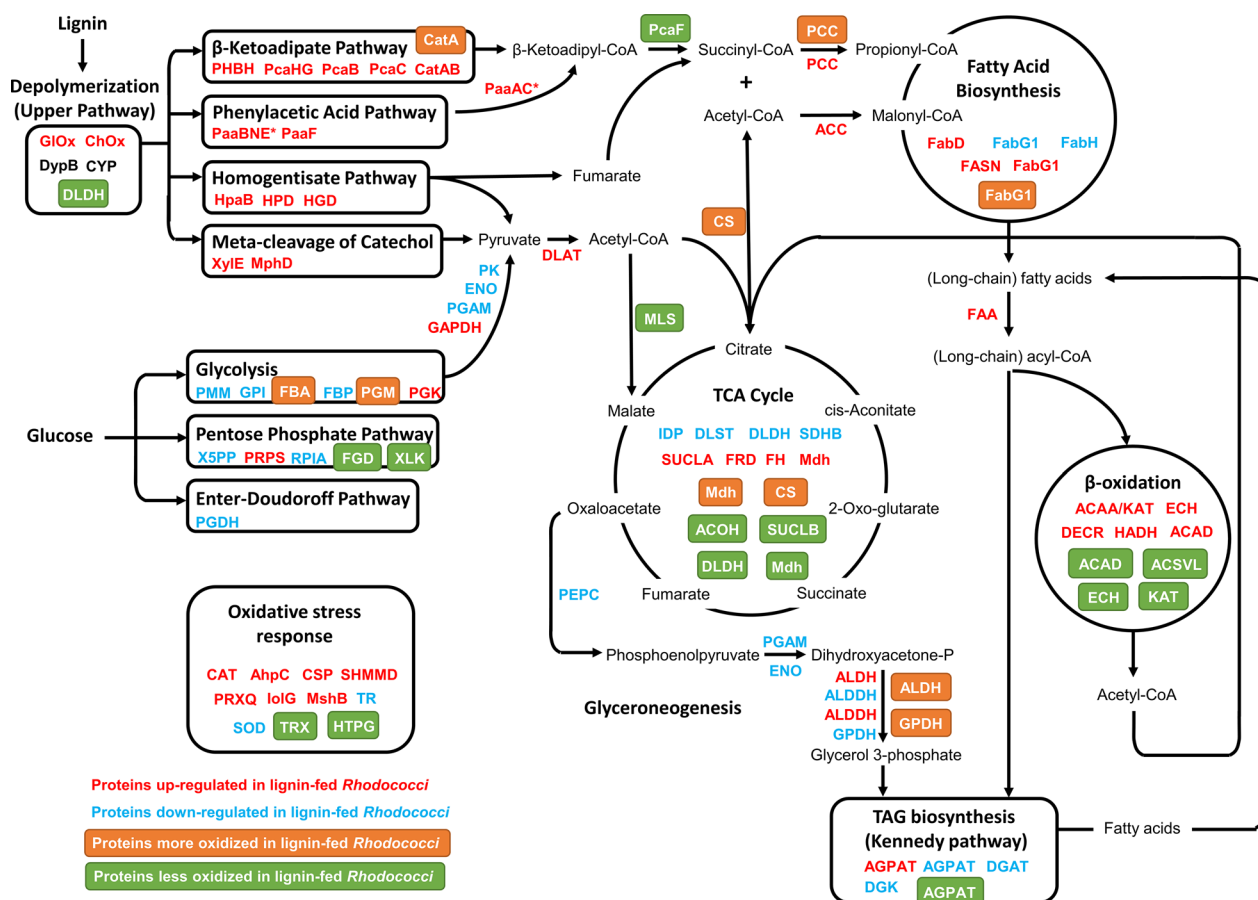
Fig. 4 Overview of main metabolic network of lignin conversion to lipid in *Rhodococci*. Compared to samples from glucose fermentation, abbreviations for proteins upregulated in lignin-fed *Rhodococci* are presented in red (* indicates that the given protein was significantly upregulated in our previous [9] work), whereas downregulated proteins in lignin-fed *Rhodococci* are presented in blue; the abbreviations for proteins with increased oxidation levels at the reported cysteine thiols are shown in orange boxes, whereas protein cysteine sites with decreased oxidation level are shown in green boxes. Proteins written in black were observed but significant differences in expression were not

β-ketoadipyl-CoA to acetyl-CoA and succinyl-CoA. ACAA/KAT redox-regulation in plants and bacteria involves reversible formation of a disulfide bond between two catalytic cysteines [64, 65]. Under conditions conducive to oxidation, disulfide bond formation leads to a conformational change and inactivation. Active site residues for *Rhodococcus* ACAA/KAT were predicted using NCBI and UniProt sequence alignments and yielded Cys109, His401, and Cys431 [58, 66]. In our results, Cys109 was less oxidized (a free thiol instead of a disulfide bond), suggesting higher activity for fatty acid and aromatic degradation during lignin conversion.

In addition to carbon assimilation and lipid metabolism, differential oxidation of enzymes involved in amino acid and purine metabolism were observed. Amino acid and purine scavenging pathways generate energy and metabolic precursors for regeneration/synthesis of NAD and various other molecules. These pathways also provide endogenous sources of nitrogen during nitrogen limitation [2–4]. $NADP^+$-dependent succinate-semialdehyde dehydrogenase (SSADH), which is involved in glutamate degradation, catalyzes the conversion of succinate-semialdehyde to succinate and regenerates NADPH as a result. Decreased oxidation of SSADH was observed in the lignin condition hinting at a redox regulatory mechanism sensitive to the available carbon source under nitrogen limitation. This is also supported by the lower oxidation state of adenosine deaminase, involved in purine scavenging, and a putative enamine deaminase (RidA), which gets rid of reactive enamine intermediates [67, 68]. These intermediates are generated by pyridoxal 5′-phosphate-dependent enzymes such as ornithine aminotransferase and phosphoserine aminotransferase (both less oxidized in our results). Interestingly, xanthine dehydrogenase, which converts xanthine to urate, can be converted to the ROS-generating oxidase form via reversible oxidation [69]. A final example includes the first enzyme

Li *et al. Biotechnology for Biofuels and Bioproducts*   (2023) 16:180

Page 8 of 13

in the shikimate pathway, 3-deoxy-D-arabinoheptulosonate 7-phosphate synthase, which exhibited 9.01-fold lower oxidation. This pathway is important for metabolism of aromatic amino acids such as tryptophan which is required for de novo NAD synthesis [70]. These results showcase the complexity by which protein activity is regulated to modulate availability of essential nitrogenous metabolites (e.g., cofactors and amino acids).

Besides metabolic enyzmes, several transcriptional regulators were differentially oxidized, two of which belong to the two-component systems (TCS). This suggests redox regulation of TCS components which impact signal transduction and metabolism at the transcriptional level in response to environment changes such as nitrogen limitation and carbon source availability [71, 72]. The TCS response regulator GlnR is a global regulator with a central role in nitrogen metabolism. This regulator has been reported in other *Mycobacteria* [73, 74]. The transcriptional regulator NnaR, which can be activated by GlnR, is a co-activator associated with nitrate/nitrite assimilation. NnaR orthologues have been found in *R. jostii* and *R. opacus* and are named NlpR. NlpR exhibits functionality in modulating lipogenesis and lipid accumulation in addition to ammonium limitation [5]. This implies an important role of the GlnR-mediated system in lipid accumulation for oleaginous *Rhodococci*. Another TCS consisting of histidine kinase PrrB and response regulator PrrA was reported in *Mycobacterium smegmatis* and regulates expression of several genes involved in TAG and lipid biosynthesis pathways [75]. Unfortunately, little is known about redox regulation of TCS and its partners.

Redox regulation has been proposed for stress conditions such as nitrogen-limitation and even in the absence of stress [30]. It is well established that thioredoxin (Trx) and glutathione-glutaredoxin antioxidant systems mediate redox homeostasis in eukaryotes [76, 77]. The exposed active 2-Cys sites of these proteins reduce oxidized proteins via thiol-disulfide exchange reactions. Similar mechanisms were proposed for the MSH-mycoredoxin (Mrx) system in Gram-positive bacteria [44]. In our results, several proteins involved in MSH synthesis and metabolism were upregulated during lignin fermentation. Furthermore, peroxiredoxin and alkyl hydroperoxide reductases (AhpC), which are important scavengers of H_2O_2 and peroxide-functionalized molecules, were upregulated during lignin fermentation [78]. Although protein abundances of the Trx system remained unchanged or downregulated, a putative thioredoxin 2-Cys site (Cys76 and Cys79) indicated decreased oxidation level in lignin-fed samples suggesting an active antioxidant defense (Fig. 3B). Meanwhile, a chaperone protein HtpG (a bacterial homolog

of the eukaryotic chaperone Hsp90 which is involved in response to many environmental stresses) also showed decreased oxidation (up to 2.63 folds) at two Cys sites [79]. The role of these antioxidants in redox regulation of *Rhodococcus* metabolism requires further investigation.

Discussion

Our preliminary results present a pattern of putative redox-dependent protein regulation that modulates a variety of metabolic pathways and biological processes (Fig. 4). Ultimately, differences in protein redox states track well with changes in abundance for corresponding biological processes. Firstly, a number of proteins in aromatic degradation pathways increased in abundance while PcaF and MLS were less oxidized, supporting catabolism of aromatics for TCA anaplerosis. Secondly, in addition to higher oxidation of PCC and FabG, downregulation of FAS and other fatty acid synthesis enzymes hints at a reduced anabolic flux from central metabolites to lipogenesis. Thirdly, proteins involved in β-oxidation and acetyl-CoA conversion (i.e., MLS) showed higher abundance and lower oxidation (separately, given the aforementioned filter criteria) evincing increased fatty acid degradation to maintain flux to the TCA cycle. Lastly, most glyceroneogenesis and Kennedy pathway proteins showed lower abundance pointing to decreased TAG synthesis. The orchestration of these carbon metabolism modules and those detailed for nitrogen metabolism (e.g., purine scavenging/synthesis) supports a regime for generating and cycling central metabolites and energy to build and maintain cell biomass instead of accumulating lipids. This metabolic redistribution seems correlated with oxidative stress response, but a causal link was not determined. Further investigations of oxidative stress and metabolism using lignin will be required to probe these relationships.

Profiling redox PTMs is a powerful first step towards investigating their potential regulatory roles. Future research will harness molecular approaches to specify antioxidant-enzyme interactions, redox switches, and the functional consequences of redox states. Immunoprecipitation is a widely used approach to identify protein–protein interactions: this mature technology may be used to co-precipitate antioxidants and their binding partners [80, 81]. Even though limited information is available for the identified proteins, bioinformatics and modeling tools can be used to predict cysteine site exposure, which affects their reactivity [31]. Direct mutagenesis and activity assays can be used to study individual proteins of importance to elucidate functional changes caused by redox PTMs and interrogate hypothetical redox switches for metabolic regulation. Promoting reducing power generation or enhancing

Li *et al. Biotechnology for Biofuels and Bioproducts*   (2023) 16:180

Page 9 of 13

antioxidant activities during lignin conversion may also improve lipid yields in *Rhodococci*—especially for demanding carbon sources like aromatics and lignin [82]. One novel approach for regenerating reducing power could be supplementing *Rhococcus* cultures with hydrogen (perhaps from a hydrogen-producing microorganism). Our results confirm expression and differential oxidation of a cytoplasmic [NiFe(Se)]-hydrogenase [83–85].

Our study of co-cultured *Rhodococci* provides intriguing metabolic insights and a platform for discovering candidate proteins involved in redox regulatory networks. Moreover, this study exemplifies how proteomics can be used to study synthetic microbial consortia, even though sequence similarity among the strains employed herein makes this challenging [86]. In future work, we plan to explore and validate select Cys site modifications using the open search strategy with FragPipe and targeted redox proteomics methods [87, 88]. Furthermore, we endeavor to qualify mechanisms of microbial interactions using metabolomics [17, 89].

Conclusions

Efficient bacterial lipid production requires a steady carbon and energy flux to generate acetyl-CoA, glycerol-3-phosphate, and NADPH, while balancing fundamental requirements for enzyme production and cell maintenance. For lignin, we theorize that this balance is difficult to establish due to resource expenditure for enzyme production and oxidative stress response, the latter of which competes for NADPH. To study redox state as a function of carbon source, we investigated the expressed metabolisms of a synthetic *Rhodococcus* consortium grown on alkali lignin vs. glucose under nitrogen-limited conditions. A novel mass spectrometry-based detection workflow allowed us to pinpoint putative redox regulatory nodes in metabolic pathways by simultaneously quantifying protein abundances and redox states. Independent of abundance, several proteins in both conditions were differentially oxidized providing possible targets for further study. Additional studies of ROS, oxidants like lipid peroxides, and the MSH/MSSM ratio will further our understanding of redox imbalance and regulation during lignin utilization. Functional studies using targeted mutagenesis, molecular cloning, and activity assays will be required to confirm redox regulation of the reported proteins and tease out contributions to redox imbalance from lignin utilization vs. nitrogen starvation. This study exemplifies a unique perspective of microbial metabolism one can attain using redox proteomics: specifically, that PTMs are implicated in the tug-and-pull of oxidation and reduction, which lie at the heart of metabolism.

Methods

Alkali lignin preparation

Alkali-extracted lignin from corn stover was prepared as previously described [9, 18]. Briefly, lignin-rich solids containing 20% glucan, 11% xylan, 3% arabinan, 2% galactan, 53% lignin, and 11% ash were first obtained by treating corn stover with 0.1 M NaOH at 80 °C for 2 h. Then, lignin was solubilized by soaking lignin-rich solids in 0.1 M NaOH at pH 12.5 again. The supernatant was filtered filtered through 11 μm pore size Whatman filters. Lignin was recovered from the filtrate by slowly adjusting the pH to 3 with 2 M H_2SO_4. Precipitated lignin was collected and washed twice with 70 °C deionized water by filtration, then lyophilized for 3 days. Cellulose and hemicellulose fractions were not observed in the final alkali-extracted lignin [18]. The alkali lignin consisted of aromatic p-hydroxyphenyl (H), guaiacyl (G) and syringyl (S) units, and major lignin linkages (β-O-4, β-β, and β-5) as reported in the our previous work [18].

Rhodococci cultivation

Co-cultivation of three *Rhodococcus* strains (*R. opacus* PD630, *R. jostii* RHA1, and its mutant *R. jostii* RHA1 VanA-) was conducted as previously described.[1] Briefly, seed cultures for each strain were inoculated at 5% (v/v) into M9 medium with supplements and incubated at 30 °C, 180 rpm for 5 days. 5 g/L of glucose or alkali corn stover lignin was used as sole carbon sources. Ammonium sulfate was added as a nitrogen source at a C/N ratio = 15/1 (g/g). After fermentation, cells were pelleted by centrifugation, washed twice with NaCl solution (0.9%, w/v), and then processed for LC–MS/MS.

Proteomics sample preparation

After fermentation, cells were pelleted by centrifugation at $8000 \times g$ and 4 °C for 15 min, then washed twice with NaCl solution (0.9%, w/v). Cell pellets were resuspended in 10% (w/v) trichloroacetic acid (TCA) followed by incubation on ice for 20 min to partially lyse cells and preserve the redox proteome [90]. Precipitated proteins and cell debris were pelleted by centrifugation at 13,000 *g* for 15 min at 4 °C. The pellet was washed with 500 μl of ice-cold 10% TCA and then with 200 μl ice-cold 5% TCA. Then the pellet was resuspended in lysis buffer (250 mM HEPES, 10 mM EDTA, 0.5% SDS, 8 M urea, 10 mM HPE-IAM, pH 7.5) by intermittent sonication and incubation at 37 °C for 2 h [32, 90]. Bead-beating was performed using 100 μl of 0.1-mm zirconia/silica beads to further lyse cells and extract proteins. Cell lysate was centrifuged at 14,000 *g* for 10 min at 4 °C to remove cellular debris. The supernatant was incubated at 37 °C for 30 min for complete alkylation followed by acetone precipitation. The resultant protein pellet was dissolved in 25 mM

ammonium bicarbonate buffer containing 8 M urea (pH 8) then subjected to FASP Protein Digestion Kit for lignin removal and trypsin digestion. All samples were cleaned up by C18 SPE column and concentrated by a Speed Vac SC110 following the manufacturer's instructions. Samples were reconstituted to 0.1 µg/µL with 0.1% formic acid for LC–MS/MS analysis.

LC–MS/MS analysis

Three biological replicates of samples were analyzed by a nanoAcquity ultra performance liquid chromatography (UPLC) system (Waters) coupled to a Q-Exactive HF Mass Spectrometer (Thermo Scientific, San Jose, CA) as previously described [91]. Protein identification and label-free quantification (LFQ) was conducted using MaxLFQ algorithm offered by MaxQuant [92], searching against FASTA files (*R. opacus* PD630, Accession: PRJNA30413; *R. jostii* RHA1, Accession: PRJNA309609) from NCBI and JGI databases [93, 94]. Dynamic oxidation of methionine (15.9949 Da) and dynamic HPE-IAM modification of Cys (177.0790 Da) were used for searching.

Data analysis

LFQ intensities of proteins exported from MaxQuant were log2 transformed and compared by Student's t-test values adjusted for Permutation-based false discovery rate in Perseus [95]. Significant protein abundance changes met the following criteria: (a) Student's t-test q-value < 0.05; (b) fold-change > 1.5 or < −1.5. Protein redox state (i.e., oxidation states of cysteine thiols) was compared at peptide level by quantification of HPE-IAM-Cys peptides. Raw intensities of unoxidized cysteine-containing peptides (with add-on mass of HPE-IAM moiety) exported from MaxQuant were log2 transformed and normalized by median-center normalization across conditions, followed by Student's t-test in Perseus. Protein redox state was quantified at Cys site level by annotation of Cys site of individual HPE-IAM-Cys peptides and aggregation of raw intensities of peptides with the same Cys sites. Then, Cys site intensities were log2 transformed and normalized, followed by student's t-test by R. Protein cysteines with significantly increased or reduced oxidation level must pass the following criteria: (a) Student's t-test raw p-value < 0.05; (b) fold-change of Cys site intensities > 1.5 or < −1.5; (c) log2 (fold-change) of corresponding protein abundance > −1.5 and < 1.5.

Abbreviations

4GT	4-Alpha-glucanotransferase
ABCT	Carbohydrate ABC transporter ATP-binding protein, CUT1 family
ACAD	Acyl-CoA dehydrogenase
ACOH	Aconitate hydratase
ACSVL	Putative (very) long chain acyl-CoA synthase
AGDH	Putative arogenate/prephenate dehydrogenase
AGPAT	1-Acyl-sn-glycerol-3-phosphate acyltransferase
AhpC	Alkyl hydroperoxide reductase subunit C
ALDDH	Aldehyde dehydrogenase
ALDH	NAD-dependent alcohol dehydrogenase
ASADH	Aspartate-semialdehyde dehydrogenase
CAT	Catalase
CatA	Catechol 1,2-dioxygenase
CatB	Muconate cycloisomerase
CLO	Choline oxidase
CS	Citrate synthase
CSP	Cold-shock DNA-binding protein family
DGAT	Diacylglycerol O-acyltransferase
DGK	Diacylglycerol kinase
DHAD	Dihydroxy-acid dehydratase 1
DHQD	3-Dehydroquinate dehydratase
DLAT	Pyruvate dehydrogenase E2 component (dihydrolipoamide acetyltransferase)
DLDH	Dihydrolipoamide dehydrogenase
DLST	2-Oxoglutarate dehydrogenase E2 component (dihydrolipoamide succinyltransferase)
DPT	NAD⁺ diphosphatase
ECH	Enoyl-CoA hydratase
ENO	Enolase
FAA	Long-chain-fatty-acid–CoA ligase/fatty-acyl-CoA synthase
FabD	[Acyl-carrier-protein] S-malonyltransferase
FABG1	3-Oxoacyl-[acyl-carrier-protein] reductase FabG1
FabH	3-Oxoacyl-[acyl-carrier-protein] synthase 3
FASN	Fatty acid synthase
FBA	Fructose-bisphosphate aldolase
FBP	Fructose-1,6-bisphosphatase II
FGD	F420-dependent glucose-6-phosphate dehydrogenase
FH	Fumarate hydratase class I, aerobic;fumarase, class I, homodimeric
FRD	Fumarate reductase iron-sulfur subunit/fumarate reductase membrane anchor subunit/Fumarate reductase flavoprotein subunit
GAPDH	Glyceraldehyde-3-phosphate dehydrogenase
GK	Glucokinase
GPDH	Glycerol-3-phosphate dehydrogenase
GPI	Glucose-6-phosphate isomerase
HADH	3-Hydroxyacyl-CoA dehydrogenase
HGD	Homogentisate 1,2-dioxygenase
HpaB	4-Hydroxyphenylacetate 3-monooxygenase oxygenase component
HPD	4-Hydroxyphenylpyruvate dioxygenase
HTPG	Molecular chaperone HtpG
IDP	Isocitrate dehydrogenase
IMPD	IMP dehydrogenase
IolG	Myo-inositol 2-dehydrogenase/ D-chiro-inositol 1-dehydrogenase, iolG
KARI	Ketol-acid reductoisomerase
KAT/ACAA/PcaF	3-Ketoacyl-CoA thiolase/ Acetyl-CoA acetyltransferase/ β-Ketoadipate:succinyl-CoA thiolase, PcaF
M2DH	Mannitol 2-dehydrogenase
Mdh	Malate dehydrogenase (quinone)
MhpD	2-Keto-4-pentenoate hydratase/2-oxohepta-3-ene-1,7-dioic acid hydratase
MLS	Malate synthase
MshB	1D-myo-inositol 2-acetamido-2-deoxy-alpha-D-glucopyranoside deacetylase
OPCA	Glucose-6-phosphate dehydrogenase assembly protein OpcA
PaaAC	Ring 1,2-phenylacetyl-CoA epoxidase
PaaBNE	Phenylacetate-CoA oxygenase
PaaF	Phenylacetate-CoA ligase
PcaC	4-Carboxymuconolactone decarboxylase/ 3-oxoadipate enol-lactonase
PcaHG	Protocatechuate 3,4-dioxygenase
PCC	Acetyl/propionyl-CoA carboxylase, alpha subunit

PEPC	Phosphoenolpyruvate carboxykinase	
PGAM	Phosphoglycerate	mutase
	(2,3-diphosphoglycerate-dependent)	
PGDH	6-Phosphogluconate dehydrogenase	
PGK	Polyphosphate glucokinase	
PGM	Phosphoglucomutase	
PHBH	4-Hydroxybenzoate 3-monooxygenase	
PK	Pyruvate kinase	
PMM	Phosphomannomutase	
PRPS	Ribose-phosphate pyrophosphokinase	
PRXQ	Peroxiredoxin Q/BCP	
RIBF	Riboflavin biosynthesis protein ribF	
RPIA	Ribose-5-phosphate isomerase	
SDHB	Succinate dehydrogenase subunit B	
SHMMD	S-(Hydroxymethyl)mycothiol dehydrogenase	
SOD	Superoxide dismutase	
SSADH	Succinate-semialdehyde dehydrogenase	
SUCLA	Succinyl-CoA ligase [ADP-forming] subunit alpha	
SUCLB	Succinyl-CoA ligase [ADP-forming] subunit beta	
TKTL	Transketolase	
TR	Thioredoxin reductase	
TRX	Putative thioredoxin	
USPA	Nucleotide-binding universal stress protein, UspA family	
X5PP	Xylulose-5-phosphate	
XDH	CO or xanthine dehydrogenase, Mo-binding subunit	
XLK	Xylulokinase	
XylE	Catechol 2,3-dioxygenase	

Supplementary Information

The online version contains supplementary material available at https://doi.org/10.1186/s13068-023-02424-x.

> **Additional file 1: Table S1.** Global protein abundances. **Table S2.** Proteins with significantly changed abundance. **Table S3.** Quantification of unique HPE-IAM alkylated cysteine sites. **Table S4.** Cys sites with significantly changed oxidation level.

Availability of data and materials

All data generated or analyzed during this study are included in this published article and its supplementary information files.

Declarations

Ethics approval and consent to participate
Not applicable.

Consent for publication
All the authors have agreed to the publication.

Competing interests
The authors declare that they have no competing interests.

Author details
[1]Bioproducts, Sciences, and Engineering Laboratory, Department of Biological Systems Engineering, Washington State University, Richland, WA 99354, USA. [2]Biological Sciences Division, Pacific Northwest National Laboratory, Richland, WA 99352, USA.

References

1. Cappelletti M, Presentato A, Piacenza E, Firrincieli A, Turner RJ, Zannoni D. Biotechnology of *Rhodococcus* for the production of valuable compounds. Appl Microbiol Biotechnol. 2020;104:8567–94.
2. Amara S, Seghezzi N, Otani H, Diaz-Salazar C, Liu J, Eltis LD. Characterization of key triacylglycerol biosynthesis processes in *rhodococci*. Sci Rep. 2016;6:24985.
3. Alvarez HM, Herrero OM, Silva RA, Hernández MA, Lanfranconi MP, Villalba MS. Insights into the metabolism of Oleaginous *Rhodococcus* spp. Appl Environ Microbiol. 2019;85:e00498-e519.
4. Costa JSD, Herrero OM, Alvarez HM, Leichert L. Label-free and redox proteomic analyses of the triacylglycerol-accumulating *Rhodococcus jostii* RHA1. Microbiology. 2015;161:593–610.
5. Hernández MA, Gleixner G, Sachse D, Alvarez HM. Carbon allocation in *Rhodococcus jostii* RHA1 in response to disruption and overexpression of nlpR regulatory gene, based on 13C-labeling analysis. Front Microbiol. 2017;8:1992.
6. Kurosawa K, Wewetzer SJ, Sinskey AJ. Triacylglycerol production from corn stover using a xylose-fermenting *Rhodococcus opacus* Strain for lignocellulosic biofuels. Microb Biochem Technol. 2014;6:254–9.
7. Kurosawa K, Boccazzi P, de Almeida NM, Sinskey AJ. High-cell-density batch fermentation of *Rhodococcus opacus* PD630 using a high glucose concentration for triacylglycerol production. J Biotechnol. 2010;147:212–8.
8. Li X, Xu Z, Gluth A, Qian W-J, Yang B. Proteomic approaches for advancing the understanding and application of oleaginous bacteria for bioconversion of lignin to lipids. In: Lignin utilization strategies: from processing to applications. American Chemical Society; 2021. p. 61–96.
9. Li X, He Y, Zhang L, Xu Z, Ben H, Gaffrey MJ, et al. Discovery of potential pathways for biological conversion of poplar wood into lipids by co-fermentation of *Rhodococci* strains. Biotechnol Biofuels. 2019;12:60.
10. Li X, Xu Z, Cort JR, Qian W-J, Yang B. Lipid production from non-sugar compounds in pretreated lignocellulose hydrolysates by *Rhodococcus jostii* RHA1. Biomass Bioenergy. 2021;145: 105970.
11. Kosa M, Ragauskas AJ. Bioconversion of lignin model compounds with oleaginous *Rhodococci*. Appl Microbiol Biotechnol. 2012;93:891–900.
12. Le RK, Das P, Mahan KM, Anderson SA, Wells T, Yuan JS, et al. Utilization of simultaneous saccharification and fermentation residues as feedstock for lipid accumulation in *Rhodococcus opacus*. AMB Express. 2017;7:185.

Li *et al. Biotechnology for Biofuels and Bioproducts*   (2023) 16:180

Page 12 of 13

13. Kosa M, Ragauskas AJ. Lignin to lipid bioconversion by oleaginous *Rhodococci*. Green Chem. 2013;15:2070–4.

14. Kamimura N, Takahashi K, Mori K, Araki T, Fujita M, Higuchi Y, et al. Bacterial catabolism of lignin-derived aromatics: new findings in a recent decade: update on bacterial lignin catabolism. Environ Microbiol Rep. 2017;9:679–705.

15. Ahmad M, Roberts JN, Hardiman EM, Singh R, Eltis LD, Bugg TDH. Identification of DypB from *Rhodococcus jostii* RHA1 as a lignin peroxidase. Biochemistry. 2011;50:5096–107.

16. Erickson E, Bleem A, Kuatsjah E, Werner AZ, DuBois JL, McGeehan JE, et al. Critical enzyme reactions in aromatic catabolism for microbial lignin conversion. Nat Catal. 2022;5:86–98.

17. Lin L. Bottom-up synthetic ecology study of microbial consortia to enhance lignocellulose bioconversion. Biotechnol Biofuels Bioprod. 2022;15:14.

18. He Y, Li X, Ben H, Xue X, Yang B. Lipid production from dilute alkali corn stover lignin by *Rhodococcus* Strains. ACS Sustain Chem Eng. 2017;5:2302–11.

19. Chen H-P, Chow M, Liu C-C, Lau A, Liu J, Eltis LD. Vanillin catabolism in *Rhodococcus* jostii RHA1. Appl Environ Microbiol. 2012;78:586–8.

20. Sainsbury PD, Hardiman EM, Ahmad M, Otani H, Seghezzi N, Eltis LD, et al. Breaking down lignin to high-value chemicals: the conversion of lignocellulose to vanillin in a gene deletion mutant of *Rhodococcus jostii* RHA1. ACS Chem Biol. 2013;8:2151–6.

21. MacEachran DP, Sinskey AJ. The *Rhodococcus opacus* TadD protein mediates triacylglycerol metabolism by regulating intracellular NAD(P)H pools. Microb Cell Fact. 2013;12:104.

22. Bissaro B, Várnai A, Røhr ÅK, Eijsink VGH. Oxidoreductases and reactive oxygen species in conversion of lignocellulosic biomass. Microbiol Mol Biol Rev. 2018;82:e00029-e118.

23. Henson WR, Campbell T, DeLorenzo DM, Gao Y, Berla B, Kim SJ, et al. Multi-omic elucidation of aromatic catabolism in adaptively evolved *Rhodococcus opacus*. Metab Eng. 2018;49:69–83.

24. Lemire J, Alhasawi A, Appanna VP, Tharmalingam S, Appanna VD. Metabolic defence against oxidative stress: the road less travelled so far. J Appl Microbiol. 2017;123:798–809.

25. Costa JSD, Silva RA, Leichert L, Alvarez H. Proteome analysis reveals differential expression of proteins involved in triacylglycerol accumulation by *Rhodococcus jostii* RHA1 after addition of methyl viologen. Microbiology. 2017;163:343–54.

26. Sundararaghavan A, Mukherjee A, Sahoo S, Suraishkumar GK. Mechanism of the oxidative stress-mediated increase in lipid accumulation by the bacterium, *R. opacus* PD630: experimental analysis and genome-scale metabolic modeling. Biotechnol Bioeng. 2020;117:1779–88.

27. Zhang T, Gaffrey MJ, Li X, Qian W-J. Characterization of cellular oxidative stress response by stoichiometric redox proteomics. Am J Physiol Cell Physiol. 2021;320:C182–94.

28. Davies MJ. Protein oxidation and peroxidation. Biochem J. 2016;473:805–25.

29. Winterbourn CC. Reconciling the chemistry and biology of reactive oxygen species. Nat Chem Biol. 2008;4:278–86.

30. Shi K, Gao Z, Shi T-Q, Song P, Ren L-J, Huang H, et al. Reactive oxygen species-mediated cellular stress response and lipid accumulation in oleaginous microorganisms: the state of the art and future perspectives. Front Microbiol. 2017;8:793.

31. Duan J, Zhang T, Gaffrey MJ, Weitz KK, Moore RJ, Li X, et al. Stoichiometric quantification of the thiol redox proteome of macrophages reveals subcellular compartmentalization and susceptibility to oxidative perturbations. Redox Biol. 2020;36: 101649.

32. Li X, Day NJ, Feng S, Gaffrey MJ, Lin T-D, Paurus VL, et al. Mass spectrometry-based direct detection of multiple types of protein thiol modifications in pancreatic beta cells under endoplasmic reticulum stress. Redox Biol. 2021;46: 102111.

33. Ali HS, Henchman RH, de Visser SP. Lignin biodegradation by a cytochrome P450 enzyme: a computational study into syringol activation by GcoA. Chemistry. 2020;26:13093–102.

34. García-Hidalgo J, Ravi K, Kuré L-L, Lidén G, Gorwa-Grauslund M. Identification of the two-component guaiacol demethylase system from *Rhodococcus rhodochrous* and expression in *Pseudomonas putida* EM42 for guaiacol assimilation. AMB Express. 2019;9:34.

35. Majeke BM, Collard F-X, Tyhoda L, Görgens JF. The synergistic application of quinone reductase and lignin peroxidase for the deconstruction of industrial (technical) lignins and analysis of the degraded lignin products. Bioresour Technol. 2021;319: 124152.

36. Perna V, Meyer AS, Holck J, Eltis LD, Eijsink VGH, Wittrup AJ. Laccase-catalyzed oxidation of lignin induces production of H_2O_2. ACS Sustain Chem Eng. 2020;8:831–41.

37. Kumar M, Verma S, Gazara RK, Kumar M, Pandey A, Verma PK, et al. Genomic and proteomic analysis of lignin degrading and polyhydroxyalkanoate accumulating β-proteobacterium *Pandoraea* sp. ISTKB Biotechnol Biofuels. 2018;11:154.

38. Janusz G, Pawlik A, Sulej J, Świderska-Burek U, Jarosz-Wilkołazka A, Paszczyński A. Lignin degradation: microorganisms, enzymes involved, genomes analysis and evolution. FEMS Microbiol Rev. 2017;41:941–62.

39. Wei Z, Wilkinson RC, Rashid GMM, Brown D, Fülöp V, Bugg TDH. Characterization of thiamine diphosphate-dependent 4-hydroxybenzoylformate decarboxylase enzymes from *Rhodococcus jostii* RHA1 and *Pseudomonas fluorescens* Pf-5 involved in degradation of Aryl C_2 lignin degradation fragments. Biochemistry. 2019;58:5281–93.

40. Alruwaili A, Rashid GMM, Bugg TDH. Application of *Rhodococcus jostii* RHA1 glycolate oxidase as an efficient accessory enzyme for lignin conversion by bacterial Dyp peroxidase enzymes. Green Chem. 2023;25:3549–60.

41. Doukyu N, Ishikawa M. Cholesterol oxidase from *Rhodococcus erythropolis* with high specificity toward β-cholestanol and pytosterols. PLoS ONE. 2020;15: e0241126.

42. Ferreira P, Hernandez-Ortega A, Herguedas B, Martínez ÁT, Medina M. Aryl-alcohol oxidase involved in lignin degradation. J Biol Chem. 2009;284:24840–7.

43. Singh S, Brocker C, Koppaka V, Ying C, Jackson B, Matsumoto A, et al. Aldehyde dehydrogenases in cellular responses to oxidative/electrophilic stress. Free Radic Biol Med. 2013;56:89–101.

44. Imber M, Pietrzyk-Brzezinska AJ, Antelmann H. Redox regulation by reversible protein S-thiolation in Gram-positive bacteria. Redox Biol. 2019;20:130–45.

45. Tian K, Meng F, Meng Q, Gao Y, Zhang L, Wang L, et al. The analysis of estrogen-degrading and functional metabolism genes in *Rhodococcus equi* DSSKP-R-001. Int J Genomics. 2020;2020: e9369182.

46. White SW, Zheng J, Zhang Y-M, Rock CO. The structural biology of type II fatty acid biosynthesis. Annu Rev Biochem. 2005;74:791–831.

47. de Carvalho CCCR, Fischer MA, Kirsten S, Würz B, Wick LY, Heipieper HJ. Adaptive response of *Rhodococcus opacus* PWD4 to salt and phenolic stress on the level of mycolic acids. AMB Express. 2016;6:66.

48. Táncsics A, Szoboszlay S, Kriszt B, Kukolya J, Baka E, Márialigeti K, et al. Applicability of the functional gene catechol 1,2-dioxygenase as a biomarker in the detection of BTEX-degrading *Rhodococcus* species. J Appl Microbiol. 2008;105:1026–33.

49. Paysan-Lafosse T, Blum M, Chuguransky S, Grego T, Pinto BL, Salazar GA, et al. InterPro in 2022. Nucleic Acids Res. 2023;51:D418–27. https://doi.org/10.1093/nar/gkac993.

50. Matera I, Ferraroni M, Kolomytseva M, Golovleva L, Scozzafava A, Briganti F. Catechol 1,2-dioxygenase from the Gram-positive *Rhodococcus opacus* 1CP: quantitative structure/activity relationship and the crystal structures of native enzyme and catechols adducts. J Struct Biol. 2010;170:548–64.

51. Brandes N, Reichmann D, Tienson H, Leichert LI, Jakob U. Using quantitative redox proteomics to dissect the yeast redoxome. J Biol Chem. 2011;286:41893–903.

52. Cereijo AE, Asencion Diez MD, Dávila Costa JS, Alvarez HM, Iglesias AA. On the kinetic and allosteric regulatory properties of the ADP-glucose pyrophosphorylase from Rhodococcus jostii: an approach to evaluate glycogen metabolism in oleaginous bacteria. Front Microbiol. 2016;7:830.

53. Ganapathy U, Marrero J, Calhoun S, Eoh H, de Carvalho LPS, Rhee K, et al. Two enzymes with redundant fructose bisphosphatase activity sustain gluconeogenesis and virulence in *Mycobacterium tuberculosis*. Nat Commun. 2015;6:7912.

54. Gurumurthy M, Rao M, Mukherjee T, Rao SPS, Boshoff HI, Dick T, et al. A novel F420-dependent anti-oxidant mechanism protects *Mycobacterium tuberculosis* against oxidative stress and bactericidal agents. Mol Microbiol. 2013;87:744–55.

55. Yang X, Song J, Yan L-J. Chronic inhibition of mitochondrial dihydrolipoamide dehydrogenase (DLDH) as an approach to managing diabetic oxidative stress. Antioxidants. 2019;8:32.

56. Tyx RE, Roche-Hakansson H, Hakansson AP. Role of dihydrolipoamide dehydrogenase in regulation of raffinose transport in *Streptococcus pneumoniae*. J Bacteriol. 2011;193:3512–24.

57. Yu X, Hiromasa Y, Tsen H, Stoops JK, Roche TE, Zhou ZH. Structures of the human pyruvate dehydrogenase complex cores: a highly conserved catalytic center with flexible N-terminal domains. Structure. 2008;16:104–14.

58. The UniProt Consortium. UniProt: the universal protein knowledgebase in 2021. Nucleic Acids Res. 2021;49:D480–9. https://doi.org/10.1093/nar/gkaa1100.

59. Yan L-J, Sumien N, Thangthaeng N, Forster MJ. Reversible inactivation of dihydrolipoamide dehydrogenase by mitochondrial hydrogen peroxide. Free Radic Res. 2013;47:123–33.

60. Rahmanpour R, King LDW, Bugg TDH. Identification of an extracellular bacterial flavoenzyme that can prevent re-polymerisation of lignin fragments. Biochem Biophys Res Commun. 2017;482:57–61.

61. Brandes N, Rinck A, Leichert LI, Jakob U. Nitrosative stress treatment of *E. coli* targets distinct set of thiol-containing proteins. Mol Microbiol. 2007;66:901–14.

62. Go Y-M, Roede JR, Orr M, Liang Y, Jones DP. Integrated redox proteomics and metabolomics of mitochondria to identify mechanisms of Cd toxicity. Toxicol Sci. 2014;139:59–73.

63. Okamura-Ikeda K, Ikeda Y, Tanaka K. An essential cysteine residue located in the vicinity of the FAD-binding site in short-chain, medium-chain, and long-chain acyl-CoA dehydrogenases from rat liver mitochondria. J Biol Chem. 1985;260:1338–45.

64. Kim S, Jang Y-S, Ha S-C, Ahn J-W, Kim E-J, Hong Lim J, et al. Redox-switch regulatory mechanism of thiolase from *Clostridium acetobutylicum*. Nat Commun. 2015;6:8410.

65. Pye VE, Christensen CE, Dyer JH, Arent S, Henriksen A. Peroxisomal plant 3-Ketoacyl-CoA thiolase structure and activity are regulated by a sensitive redox switch. J Biol Chem. 2010;285:24078–88.

66. NCBI Resource Coordinators. Database resources of the National Center for Biotechnology Information. Nucleic Acids Res. 2013;41:D8-20. https://doi.org/10.1093/nar/gks1189.

67. Irons JL, Hodge-Hanson K, Downs DM. RidA proteins protect against metabolic damage by reactive intermediates. Microbiol Mol Biol Rev. 2020;84:e00024-e120.

68. Borchert AJ, Downs DM. The response to 2-aminoacrylate differs in *Escherichia coli* and *Salmonella enterica*, despite shared metabolic components. J Bacteriol. 2017;199:e00140-e217.

69. Nishino T. The conversion of xanthine dehydrogenase to xanthine oxidase and the role of the enzyme in reperfusion injury. J Biochem. 1994;116:1–6.

70. Boshoff HIM, Xu X, Tahlan K, Dowd CS, Pethe K, Camacho LR, et al. Biosynthesis and recycling of nicotinamide cofactors in *Mycobacterium tuberculosis*. J Biol Chem. 2008;283:19329–41.

71. Husain M, Jones-Carson J, Song M, McCollister BD, Bourret TJ, Vázquez-Torres A. Redox sensor SsrB Cys[203] enhances *Salmonella* fitness against nitric oxide generated in the host immune response to oral infection. Proc Natl Acad Sci U S A. 2010;107:14396–401.

72. Tiwari N, López-Redondo M, Miguel-Romero L, Kulhankova K, Cahill MP, Tran PM, et al. The SrrAB two-component system regulates *Staphylococcus aureus* pathogenicity through redox sensitive cysteines. Proc Natl Acad Sci U S A. 2020;117:10989–99.

73. Amon J, Bräu T, Grimrath A, Hänßler E, Hasselt K, Höller M, et al. Nitrogen control in *Mycobacterium smegmatis*: nitrogen-dependent expression of ammonium transport and assimilation proteins depends on the OmpR-type regulator GlnR. J Bacteriol. 2008;190:7108–16.

74. Malm S, Tiffert Y, Micklinghoff J, Schultze S, Joost I, Weber I, et al. The roles of the nitrate reductase NarGHJI, the nitrite reductase NirBD and the response regulator GlnR in nitrate assimilation of *Mycobacterium tuberculosis*. Microbiology. 2009;155:1332–9.

75. Maarsingh JD, Haydel SE. *Mycobacterium smegmatis* PrrAB two-component system influences triacylglycerol accumulation during ammonium stress. Microbiology. 2018;164:1276–88.

76. Wu C, Liu T, Chen W, Oka S, Fu C, Jain MR, et al. Redox regulatory mechanism of transnitrosylation by thioredoxin. Mol Cell Proteomics. 2010;9:2262–75.

77. Go Y-M, Roede JR, Walker DI, Duong DM, Seyfried NT, Orr M, et al. Selective targeting of the cysteine proteome by thioredoxin and glutathione redox systems. Mol Cell Proteomics. 2013;12:3285–96.

78. Parsonage D, Karplus PA, Poole LB. Substrate specificity and redox potential of AhpC, a bacterial peroxiredoxin. Proc Natl Acad Sci U S A. 2008;105:8209–14.

79. Grudniak AM, Markowska K, Wolska KI. Interactions of *Escherichia coli* molecular chaperone HtpG with DnaA replication initiator DNA. Cell Stress Chaperones. 2015;20:951–7.

80. Berggård T, Linse S, James P. Methods for the detection and analysis of protein–protein interactions. Proteomics. 2007;7:2833–42.

81. Stöcker S, Maurer M, Ruppert T, Dick TP. A role for 2-Cys peroxiredoxins in facilitating cytosolic protein thiol oxidation. Nat Chem Biol. 2018;14:148–55.

82. Xu P, Qiao K, Stephanopoulos G. Engineering oxidative stress defense pathways to build a robust lipid production platform in *Yarrowia lipolytica*. Biotechnol Bioeng. 2017;114:1521–30.

83. Greening C, Berney M, Hards K, Cook GM, Conrad R. A soil actinobacterium scavenges atmospheric H_2 using two membrane-associated, oxygen-dependent [NiFe] hydrogenases. Proc Natl Acad Sci U S A. 2014;111:4257–61.

84. Shafaat HS, Rüdiger O, Ogata H, Lubitz W. [NiFe] hydrogenases: a common active site for hydrogen metabolism under diverse conditions. Biochim Biophys Acta Bioenerg. 2013;1827:986–1002.

85. Salusjärvi L, Ojala L, Peddinti G, Lienemann M, Jouhten P, Pitkänen J-P, et al. Production of biopolymer precursors beta-alanine and L-lactic acid from CO_2 with metabolically versatile *Rhodococcus opacus* DSM 43205. Front Bioeng Biotechnol. 2022;10: 989481.

86. Großkopf T, Soyer OS. Synthetic microbial communities. Curr Opin Microbiol. 2014;18:72–7.

87. Kong AT, Leprevost FV, Avtonomov DM, Mellacheruvu D, Nesvizhskii AI. MSFragger: ultrafast and comprehensive peptide identification in mass spectrometry–based proteomics. Nat Methods. 2017;14:513–20.

88. Li X, Gluth A, Zhang T, Qian W-J. Thiol redox proteomics: characterization of thiol-based post-translational modifications. Proteomics. 2023;23:2200194.

89. McCarty NS, Ledesma-Amaro R. Synthetic biology tools to engineer microbial communities for biotechnology. Trends Biotechnol. 2019;37:181–97.

90. Guo J, Nguyen AY, Dai Z, Su D, Gaffrey MJ, Moore RJ, et al. Proteome-wide light/dark modulation of thiol oxidation in cyanobacteria revealed by quantitative site-specific redox proteomics. Mol Cell Proteomics. 2014;13:3270–85.

91. Zhang T, Gaffrey MJ, Thomas DG, Weber TJ, Hess BM, Weitz KK, et al. A proteome-wide assessment of the oxidative stress paradigm for metal and metal-oxide nanomaterials in human macrophages. NanoImpact. 2020;17:100194.

92. Cox J, Hein MY, Luber CA, Paron I, Nagaraj N, Mann M. Accurate proteome-wide label-free quantification by delayed normalization and maximal peptide ratio extraction. Termed MaxLFQ Mol Cell Proteomics. 2014;13:2513–26.

93. Sayers EW, Bolton EE, Brister JR, Canese K, Chan J, Comeau DC, et al. Database resources of the national center for biotechnology information. Nucleic Acids Res. 2022;50:D20–6. https://doi.org/10.1093/nar/gkab1112.

94. Nordberg H, Cantor M, Dusheyko S, Hua S, Poliakov A, Shabalov I, et al. The genome portal of the Department of Energy Joint Genome Institute: 2014 updates. Nucleic Acids Res. 2014;42:D26-31. https://doi.org/10.1093/nar/gkt1069.

95. Tyanova S, Temu T, Sinitcyn P, Carlson A, Hein MY, Geiger T, et al. The Perseus computational platform for comprehensive analysis of (prote)omics data. Nat Methods. 2016;13:731–40.

Publisher's Note